Langmuir Turbulence and Suprathermal Electron Production from the Two-Plasmon-Decay Instability Driven by Crossed Laser Beams in an Inhomogeneous Plasma

It is currently a time of great anticipation for inertial confinement fusion (ICF) research. An attempt to demonstrate ignition will likely be made at the National Ignition Facility (NIF) within the year.[1] Ignition will be attempted first in indirect-drive geometry (where the laser energy is first converted to soft x rays that drive the target), with an attempt in direct-drive geometry (where the laser directly illuminates the target) likely to occur later. In both approaches, uncertainties with regard to laser–plasma instabilities remain a serious concern. This article presents new results regarding two-plasmon-decay (TPD) instability, which is perhaps the most-serious instability for direct-drive ICF targets. TPD instability is the decay of a laser photon into two Langmuir waves (plasmons). The plasma turbulence driven by TPD produces suprathermal electrons, which can preheat the target, reducing its compressibility and negatively impacting performance.[2–4] While TPD instability has been unambiguously observed in recent direct-drive experiments (at LLE's OMEGA Laser Facility), in which diagnostic evidence includes the simultaneous observation of odd half-harmonic radiation and hard x rays attributable to hot-electron generation,[5] it is not currently possible to test at the NIF scale. This makes the calculation of hot-electron generation by TPD in relevant parameter regimes highly valuable.

In previous papers, we have studied two nonlinear models of TPD in regimes relevant to the LLE experiments: (1) the extended Zakharov model (*ZAK*)—a reduced fluid-like model with no nonlinear kinetic effects,[6–8] and (2) the fully kinetic reduced-description particle-in-cell (RPIC) model.[9] It is noted here that the *ZAK* model has been derived directly from the RPIC model as a limiting case, primarily for weak laser drives.[9] The significant nonlinear processes, noted in Ref. 9, included Langmuir decay instability (LDI), wherein the TPD Langmuir waves (LW's) parametrically decay into another LW and an ion-acoustic wave (IAW). The RPIC simulations in Ref. 9 showed significant kinetic effects, such as hot-electron generation by the excited Langmuir turbulence.

This article presents new results concerning TPD instability having three key novel components. First, TPD is excited by overlapped (crossed) laser beams, which is a generic and important feature of directly driven ICF.[9,10] Second, it includes the effects of plasma inhomogeneity. Finally, the TPD-generated flux of suprathermal electrons and their energy spectrum are explicitly computed (tolerable levels of preheat in direct-drive designs at the NIF scale are at a level of 400 J). Included in the results is a detailed description of the structure of the nonlinear state of LW turbulence that will facilitate the construction of further-reduced models. These results have been made possible by extending the RPIC model[9] to include these effects. The Zakharov model applied to inhomogeneous plasmas[7,11] predicted, in addition to nonlinear effects mentioned above,[6–8] significant electron-density profile modification caused by the ponderomotive pressure of the LW's; this modification moved the ensuing turbulent region from densities near $n_c/4$ [$n_c = m_e\omega_0^2/(4\pi e^2)$ is the critical density] to densities that were sufficiently low enough to stabilize TPD by Landau damping (the so-called Landau cutoff). This profile modification occurs on an ion-acoustic time scale and requires integration times of several tens of picoseconds (ps). The identification of the primary TPD LW's and secondary nonlinear fluctuations, such as those caused by LDI, involves the Fourier spectra of the LW envelope and low-frequency electron-density fields, similar to the procedure in Ref. 9, and will be demonstrated elsewhere.[12]

For all of the two-dimensional (2-D) simulations considered here, the plasma consisted of a linear gradient with electron density n_e/n_c varying from 0.19 to 0.27 over an axial (x) extent of 45 μm, resulting in a gradient scale length $L_n \approx 130$ μm. The transverse (y) extent of the plasma was 10 μm and the temperatures $T_{e0} = 2$ keV and $T_{i0} = 1$ keV. The incident pump laser light consisted of spatially uniform plane waves propagating at angles ±23° with respect to the x axis, each with a fluence of I_0 and wavelength $\lambda_0 = 351$ nm, with polarizations in the x–y plane. The linear density gradient under consideration was compatible with the frequency envelope representation of the LW fields because the electron-plasma frequency varied by ~±4% about the reference envelope frequency, chosen to be in the center of the simulation domain for which $n_e/n_c = 0.23$. The linear energy growth rate γ versus (beamlet) fluence I_0 was

obtained from a series of RPIC simulations in which only I_0 was varied. A very good fit to these data is given by the best-fit empirical expression $\gamma(I_0) = \gamma_0\left(I_0/I_{\text{thres}} - 1\right)$, where $I_{\text{thres}} \approx 1 \times 10^{15}$ W/cm^2 and $\gamma_0 \approx 5.8$ ps^{-1}. A more-detailed discussion of the RPIC thresholds and the influence of discrete particle effects will be given elsewhere.[12] It is observed in all of our RPIC simulations that above threshold $\left(I_0/I_{\text{thres}} > 1\right)$, Langmuir cavitation and collapse are observed at very early times (comparable to the e-folding time of the linear TPD growth), even for cases just above the TPD threshold, and appear to be primarily responsible for suprathermal electron production and nonlinear saturation of TPD.

A representative RPIC simulation with $I_0/I_{\text{thres}} = 2$ is analyzed in detail to illustrate our results. To quantify whether Langmuir cavitation actually occurs, we compute the "caviton correlator" (Ref. 13):

$$C(x,t) = \left\langle -\delta n \left| E_{\text{LW}} \right|^2 \right\rangle_y \Big/ \left[\left\langle \left\langle \delta n \right\rangle_y^{1/2} \left\langle \left| E_{\text{LW}} \right| \right\rangle_y^2 \right]_y,$$

where the operator $\langle\,\rangle_y$ denotes averaging in the transverse (y) direction, δn is the low-frequency electron-density perturbation, and E_{LW} is the LW field envelope. A *caviton* is essentially a local maximum of $\left|E_{\text{LW}}\right|^2$, spatially coincident with a local minimum of δn (i.e., $\delta n < 0$). Figure 127.1 plots $C(x,t)$, $E_{\text{LW}}(x,y)$, and $\delta n(x,y)$ at $t = 20$ ps. The solid curve on the top panel represents the spatiotemporal evolution of the quarter-critical surface. The boxes in the middle and bottom panels mark regions where Langmuir cavitation and collapse will be examined in greater spatial detail (see Fig. 127.3). As indicated in the top panel of Fig. 127.1, Langmuir cavitation and collapse are observed within a short time ($t < 1$ ps) and are observed to be accompanied by the production of suprathermal electrons after a short delay ($\tau < 2$ ps), leading to nonlinear saturation of TPD, while throughout this process, the IAW's

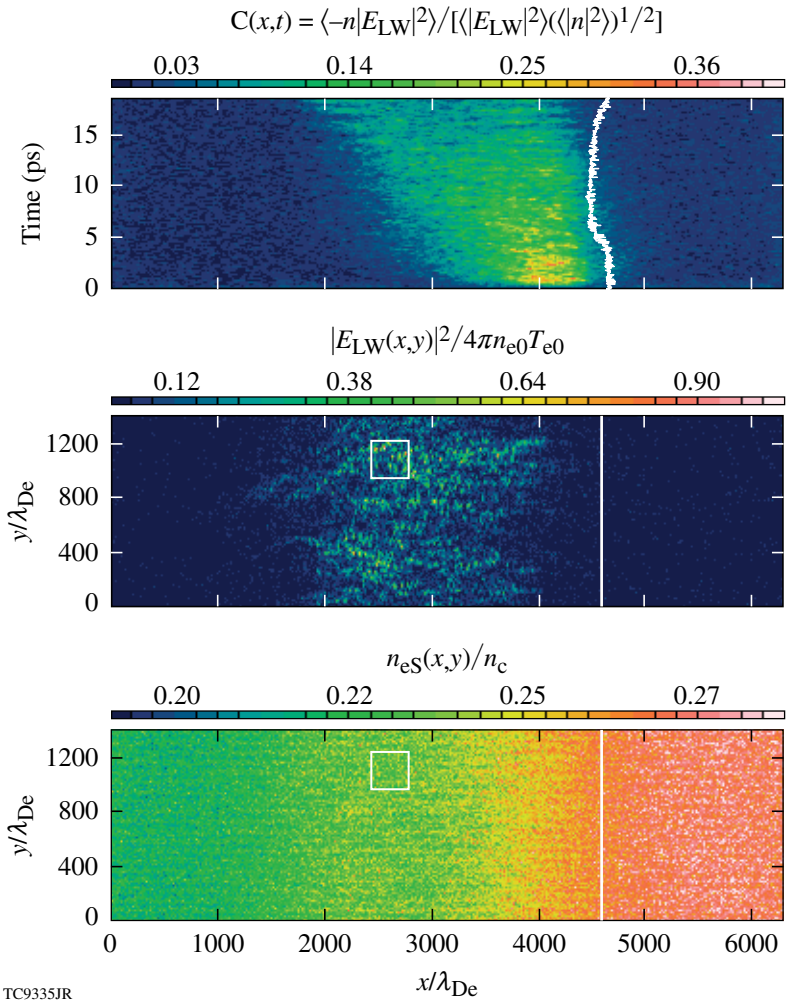

Figure 127.1
Plots of the caviton correlator $C(x,t)$, LW energy density, and the low-frequency density fluctuation at $t = 20$ ps. The solid curve on the top panel represents the spatiotemporal evolution of the quarter-critical surface. The boxes in the middle and bottom panels mark regions where Langmuir cavitation and collapse will be examined in greater spatial detail (see Fig. 127.3). Langmuir cavitation and collapse are observed to occur for $2000 < x/\lambda_{\text{De}} < 4000$.

participating in LDI have weak Fourier spectral amplitudes. The ponderomotive beating of the obliquely propagating laser waves produces a standing-wave pattern, which manifests itself as density channels on the background plasma seen in the bottom panel of Fig. 127.1. Langmuir cavitation and collapse occur preferentially in these density channels and in sufficiently strongly driven cases, can lead to "kinking" of these initially straight channels, perhaps signaling that the channels will self-focus or filament in three-dimensional (3-D) simulations. Plots of the caviton correlation as a function of density and time (not shown) indicate that LW activity peaks at $n_e/n_c \sim 0.24$, where the forward TPD LW's become degenerate and overlap for laser-propagation angles of ±23° and $T_{e0} = 2$ keV (Refs. 9–12). In addition to $C(x,t)$ shown in Fig. 127.1, which indicates that all Langmuir cavitation and collapse occur in the active region $2000 < x/\lambda_{De} < 4000$, one can perform a statistical analysis by defining (for the purposes of this study) a caviton as a spatial local maximum of $|E_{LW}(x,y)|^2$ that exceeds 10× the average LW energy density in the active region. All local maxima identified as cavitons by this criterion are plotted as a caviton-distribution function versus the normalized LW energy density $|E_{LW}|^2/4\pi n_{e0}T_{e0}$. Interestingly, it is found that cavitons follow Gaussian statistics for all RPIC simulations under consideration at each given time. In addition, the heated-electron distribution is found to be bi-Mawellian. As an example, caviton statistics and the heated-electron–distribution function, at $t =$ 13 ps, for the simulation described in Fig. 127.1, are shown in Fig. 127.2. The average LW energy density in the active region is $\langle |E_{LW}|^2 \rangle / 4\pi n_{e0}T_{e0} \sim 0.05$, and cavitons are distributed according to $F(|E_{LW}|^2) \propto \exp(-|E_{LW}|^2/4\pi n_{e0}T_{e0}\epsilon)$, where $\epsilon \approx 0.135$. The v_y-averaged electron distribution shows a bi-Maxwellian distribution with a bulk temperature of $T_{bulk} \approx$ 1.1 $T_{e0} = 2.2$ keV (slightly heated above T_{e0}) and a suprathermal electron temperature $T_{hot} \approx 30\ T_{e0} = 60$ keV. It is observed that T_{hot} depends on the strength of the laser drive and not on the kinetic energy associated with the phase velocity of the primary LW.

The electric-field intensity $|E(x,y)|^2$ is very spiky, with about 10^4 cavitons (by the above criterion) present in the active region at any given time after the system reaches saturation. Some of these cavitons can proceed to collapse and "burn out," wherein all the electrostatic energy is given up to accelerated electrons. It has been argued that in 2-D, cavitons must gather a finite amount of electrostatic energy before collapse can occur, whereas in 3-D, this threshold energy is zero. In 3-D, collapse events are expected to be weaker but more numerous.[14] Magnification of a spatial region where caviton activity is observed is shown in Fig. 127.3. Several stages of the nucleation–collapse–burnout caviton cycle are observed simultaneously. Frequency spectral diagnostics of the LW envelope fields were employed in corresponding *ZAK* simulations, which show significant LW energy for frequencies below the local electron-plasma frequency—an unambiguous signature of collapse.[13,14] Finally, the time history of the suprathermal heat flux through simulation boundaries indicates that the simulation is slowly approaching a nonlinear saturated state with ~1.5% of the input laser fluence converted into suprathermal heat flux at 20 ps.

In summary, we have performed a number of RPIC simulations with varying laser fluences for the parameters listed above. Our simulations, spanning a wide range of laser fluences $(I_0/I_{thres} = 1 \text{ to } 4)$, indicate the following salient features, which are also qualitatively observed in Zakharov simulations[12] and quasi-linear Zakharov simulations.[15] First, the ponderomotive beating of the crossed laser beams creates a standing wave

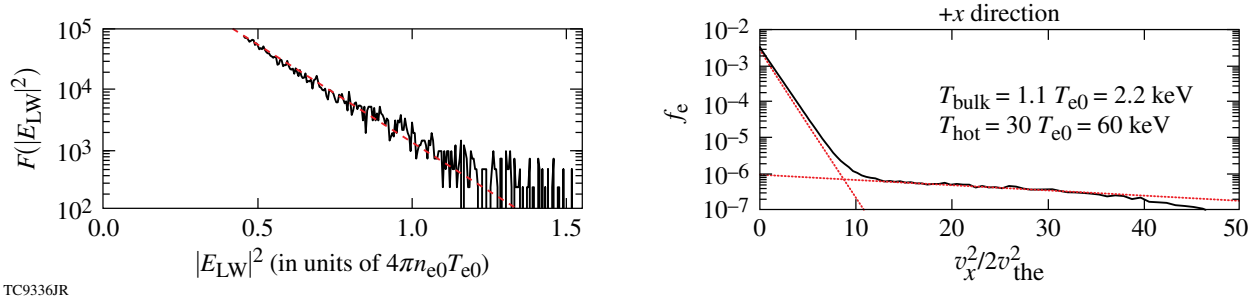

Figure 127.2
Caviton statistics and the heated-electron–distribution function at $t = 13$ ps. The spatial average LW energy density in the active region is $\langle |E_{LW}|^2 \rangle / 4\pi n_{e0}T_{e0} \sim 0.04$, and cavitons follow the distribution $F(|E_{LW}|^2) \propto \exp(-|E_{LW}|^2/4\pi n_{e0}T_{e0}\epsilon)$, where $\epsilon \approx 0.135$. The total number of cavitons $N = \int_{\varepsilon_{min}}^{\infty} F(|E_{LW}|^2)\, d(|E_{LW}|^2)$. The v_y-averaged electron distribution shows a bi-Maxwellian distribution with a bulk temperature of $T_{bulk} \approx 1.1\ T_{e0} = 2.2$ keV (slightly heated above the initial temperature) and a suprathermal electron temperature $T_{hot} \approx 30\ T_{e0} = 60$ keV.

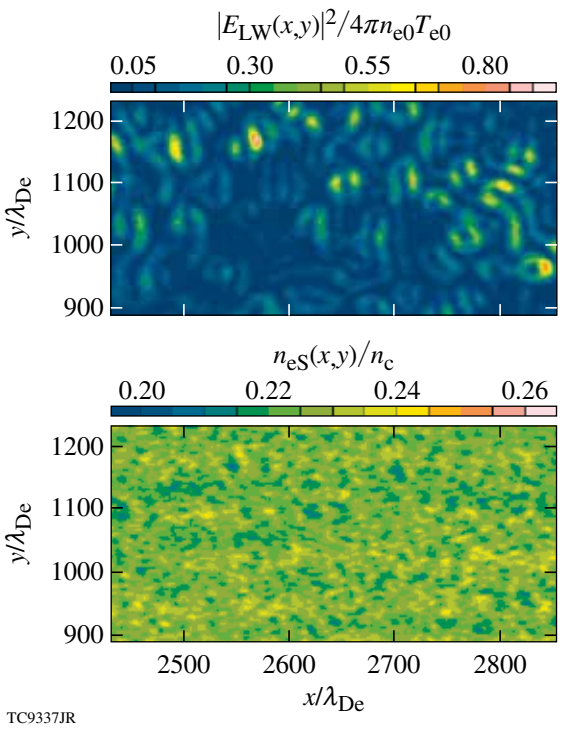

Figure 127.3
Magnification of a spatial region where caviton activity is observed (marked by the boxes in the middle and bottom panels of Fig. 127.1). Several stages of nucleation and collapse are observed simultaneously.

pattern, manifested as density channels in which Langmuir cavitation and collapse preferentially occur. Second, Langmuir cavitation and collapse occur at early times ($t < 1$ ps), accompanied by suprathermal electron production and nonlinear saturation of TPD. These observations lead us to the preliminary conclusion that LDI, which is observed in the low-frequency density-fluctuation spectrum for stronger drive, plays a secondary role in the nonlinear saturation of TPD in the regimes studied here. (A more-complete understanding of the competition of cavitation, collapse, and LDI, along with their contribution to electron acceleration, warrants further study.) Third, cavitons are shown to follow Gaussian statistics, a general observation in both RPIC and *ZAK* simulations, regardless of drive strength (as long as the drives are sufficiently strong to cause Langmuir cavitation). The suprathermal electron-distribution function is observed in all cases to be bi-Maxwellian, with hot temperatures reaching 60 to 100 keV in our simulations. The suprathermal heat flux out of the simulation domain, normalized to the overlapped laser fluence, achieved values of 0.5% to 2% for the RPIC simulations considered here. Langmuir collapse and burnout provide the dissipation (into fast electrons) that stabilizes the system in saturation and drives the LW spectrum to the small dissipation scales at the "Landau cutoff."

ACKNOWLEDGMENT

This research was supported by the U.S. Department of Energy, Office of Inertial Confinement Fusion under Cooperative Agreement No. DE-FC52-08NA28302, the University of Rochester, and the New York State Energy Research and Development Authority, and the National Nuclear Security Agency through its High-Energy-Density Laboratory Plasmas Grant No. DE-FG52-09NA29545. The support of DOE does not constitute an endorsement by DOE of the views expressed in this article.

REFERENCES

1. S. H. Glenzer *et al.*, Phys. Rev. Lett. **106**, 085004 (2011).
2. J. A. Delettrez, V. N. Goncharov, P. B. Radha, C. Stoeckl, A. V. Maximov, T. C. Sangster, J. A. Frenje, and D. Shvarts, Bull. Am. Phys. Soc. **53**, 248 (2008).
3. V. A. Smalyuk, D. Shvarts, R. Betti, J. A. Delettrez, D. H. Edgell, V. Yu. Glebov, V. N. Goncharov, R. L. McCrory, D. D. Meyerhofer, P. B. Radha, S. P. Regan, T. C. Sangster, W. Seka, S. Skupsky, C. Stoeckl, B. Yaakobi, J. A. Frenje, C. K. Li, R. D. Petrasso, and F. H. Séguin, Phys. Rev. Lett. **100**, 185005 (2008).
4. B. Yaakobi, C. Stoeckl, W. Seka, J. A. Delettrez, T. C. Sangster, and D. D. Meyerhofer, Phys. Plasmas **12**, 062703 (2005).
5. W. Seka, D. H. Edgell, J. F. Myatt, A. V. Maximov, R. W. Short, V. N. Goncharov, and H. A. Baldis, Phys. Plasmas **16**, 052701 (2009).
6. D. F. DuBois, D. A. Russell, and H. A. Rose, Phys. Rev. Lett. **74**, 3983 (1995).
7. D. A. Russell and D. F. DuBois, Phys. Rev. Lett. **86**, 428 (2001).
8. D. A. Russell, D. F. DuBois, and H. X. Vu, presented at the Workshop on SRS/SBS Saturation, Livermore, CA, 2–5 April 2002.
9. H. X. Vu, D. F. DuBois, D. A. Russell, and J. F. Myatt, Phys. Plasmas **17**, 072701 (2010).
10. R. W. Short, Bull. Am. Phys. Soc. **54**, 144 (2009).
11. J. F. Myatt, J. Zhang, J. A. Delettrez, A. V. Maximov, R. W. Short, W. Seka, D. H. Edgell, D. F. DuBois, D. A. Russell, and H. X. Vu, "The Dynamics of Hot-Electron Heating in Direct-Drive Implosion Experiments Due to the Two-Plasmon-Decay Instability," submitted to Physics of Plasmas.
12. H. X. Vu, D. F. DuBois, J. F. Myatt, and D. A. Russell, "Kinetic Simulations of the Nonlinear Evolution of the Two-Plasmon-Decay Instability in an Inhomogeneous Plasma," to be submitted to Physics of Plasmas.
13. D. F. DuBois, H. A. Rose, and D. A. Russell, Phys. Scr. **T63**, 16 (1996).
14. D. F. Dubois *et al.*, J. Geophys. Res. **98**, 17,543 (1993).
15. K. Y. Sanbonmatsu *et al.*, Phys. Plasmas **7**, 2824 (2000) and references therein.